Ab initio tight-binding analysis of CdS nanocrystals

Chad E. Junkermeier* and James P. Lewis
Department of Physics, West Virginia University, Morgantown, West Virginia 26506, USA

Garnett W. Bryant
National Institute of Standards and Technology, 100 Bureau Drive, Stop 8423, Gaithersburg, Maryland 20899-8423, USA
(Received 7 December 2007; revised manuscript received 21 April 2008; published 23 May 2008)

Spherical Cd_nS_m nanocrystals are studied via an *ab Initio* tight-binding analysis. Starting from the bulk zinc-blende structure, these nanocrystals undergo relaxation as the geometries optimize to configurations that minimize internal forces. The resulting electronic structure and molecular orbitals are analyzed and compared to the electronic structure and molecular orbitals found in the bulklike zinc-blende structure. We conclude that the states found in the gap between the valence band and the conduction band are mainly on the surface of the nanocrystals and are due to the unpassivated bonds that remain after surface relaxation.

DOI: 10.1103/PhysRevB.77.205125 PACS number(s): 73.22.−f, 61.46.Bc

I. INTRODUCTION

Semiconductor nanocrystals are small crystallites or clusters, which typically have a lattice structure close to the bulk lattice structure, that are intermediate between bulk semiconductors and molecules with regard to the electronic structure. As the number of atoms in the nanocrystal increases, the discrete energies of the molecular orbitals merge toward a pseudo continuum of energy levels that converges to the solid state band structure of the bulk material. The energy difference between the highest occupied molecular orbital (HOMO) and the lowest unoccupied molecular orbital (LUMO) decreases with increasing number of atoms. This change in the HOMO-LUMO gap as the size of the crystal changes is known as the quantum size effect.[1] Nanocrystals function as artificial atoms due to their discrete electronic spectra, which can be precisely tailored via the quantum size effect. The use of nanocrystals is being intensely explored for a wide range of optical, electronic, and quantum technologies that require systems with discrete spectra.[2]

Because a large proportion of the atoms in a nanocrystal belongs to the surface, many important physical and chemical properties may be explained in terms of the surface conformation. In an unpassivated nanocrystal, states appear in the band gap. It is commonly held that these states represent the dangling bonds of surface atoms where there is no hybridization satisfied either through passivating agents, typically organic molecules, or through surface reconstruction. Although we expect the transition probability into these surface states to be small, they may affect the quantum efficiency of the nanoparticles.

In spite of the importance of the gap states, only a few works that used first principles calculations to relax the molecular structure of the nanocrystals have been published; this is because these calculations are difficult to do except for small systems. Extensive work has been performed on CdSe and ZnSe nanocrystals, including semiempirical tight-binding methods[3–9] and density functional theory (DFT) methods.[10–14] *Ab Initio* work has been performed on CdSe, but smaller systems have been investigated.[15–17] Several groups have used either a semiempirical tight-binding model to simulate CdS systems ranging from diatomic molecules to 10 000 atom systems[18,19] or have modeled systems with less than 200 atoms by using *ab Initio* calculations.[20,21]

CdS is a component of a variety of nanoheterostructures, including CdS/HgS/CdS quantum-dot quantum wells, which are interesting for infrared applications,[22] and ZnS/CdS core-shell quantum dots, which are important for blue-green applications.[23,24] The tight-binding theory shows that strain due to lattice mismatch is important in core-shell structures.[24] However, the additional contribution by strain effects due to surface relaxation has not been determined for these CdS nanoheterostructures. Previously, we investigated gap states in large passivated and unpassivated CdS and CdS-ZnS core-shell nanocrystals by using empirical tight-binding models without strain[19] to better understand how passivation and cap layers influence the contribution of gap states to the optical response. These calculations were done by using an unrelaxed bulk lattice structure. To understand how surface reconstruction and the resulting internal lattice relaxation affect these results, we now extend these calculations to consider fully relaxed small CdS nanocrystals. In this work, we report results that have been obtained for CdS nanocrystals using a state-of-the-art *ab Initio* tight-binding method, which is known as the FIREBALL method. Our approach uses judicious approximations so that the electronic structure properties of larger nanocrystal systems can be calculated by using a tight-binding approach but with *ab Initio* Hamiltonian matrix elements. With our method, we predict the atomic rearrangement of nanocrystal particles which occurs due to surface reconstruction and lattice relaxation and determine how this influences the quantum size effect.

This paper is organized as follows. In Sec. II, we discuss the computational methods used in this work. In Sec. III, we discuss the band structure of bulk CdS. In Sec. IV, we discuss the rearrangement of the ions as we partially passivate them through relaxation. Section V discusses the effect that the surface relaxation has on the molecular orbitals of the nanocrystals. Sections VI and VII are the summary and acknowledgments, respectively.

II. COMPUTIONAL METHODS

The theoretical basis of the FIREBALL method is the use of the DFT with the charge density expanded in terms of local orbitals obtained from a pseudopotential scheme to perform molecular dynamics (MD) simulations; a summary of the method is given here and we refer the reader to Refs. 25 and 26 and references therein for a more detailed description. FIREBALL can perform several different types of calculations based on the method chosen and the approximations used to compute the Hamiltonian matrix elements. For this work, we used two types of density functionals, the Harris functional[27] and the functional of Demkov *et al.*,[28] the use of which we will shortly discuss. We use the Horsfield exchange-correlation approximation, which gives accurate results when working with solids that are not in a close pack geometry or with molecules.[25,29]

In this work, we will be using MD simulations to relax the surface structure of nanocrystals. Because FIREBALL is a DFT code, we compute the potentials acting on each atom from the Hamiltonian. In order for the Hamiltonian to have the correct form, we must first solve the one-electron Schrödinger equation. To do so, we use a minimal basis set of local orbitals with Hamann-type pseudopotentials.[30] The wave function of each local orbital is defined to vanish at a cutoff radius (similar to an "atom in a box"). The restricted radial range of the orbitals simplifies the computation of matrix elements because the overlap integrals used in defining various interactions (i.e., Coulomb-Coulomb and exchange correlation) are zero everywhere outside of the cutoff radius.

In both the Harris functional and Demkov–Ortega–Sankey–Grumbach (DOGS), the input density is a sum of confined spherical atomiclike densities, $\rho_{in}(\mathbf{r})=\Sigma_i n_i|\phi_i(\mathbf{r}-\mathbf{R}_i)|^2$.[28] The basis functions $\phi_i(\mathbf{r}-\mathbf{R}_i)$ are found by solving the one-electron Schrödinger equation. They are computed beforehand and do not change over the course of a MD calculation. The n_i are the occupation numbers of the "atomic" orbitals. The Harris functional is similar to the Kohn–Sham functional except that it usually gives a better approximation to the ground state energy when the density ρ is not self-consistently derived. When using the Harris functional in FIREBALL, the n_i have integer values related to the number of valence electrons in the respective shells of the neutral atom. With DOGS the occupation numbers start out in the neutral atom configuration but self-consistently change to noninteger quantities to allow for charge transfer between atoms, with the total charge of the system being conserved.

A semiconducting nanocrystal should have a "gap" in the energy of the internally confined states that is larger than the bulk band gap. These gaps are expected to vary in size with the number of atoms within the nanocrystal. In a perfect crystal, the band gap would be defined as the energy difference between the valence band edge state and the conduction-band edge state. In a nanocrystal with no dangling bonds, the HOMO state is the highest internally confined state and the LUMO is the next unoccupied state. Dangling bonds produce molecular orbital states that fall around and within the band-gap region; thus, the HOMO may be above the highest occupied internally confined valence band state. We will hereafter refer to the internally confined state at the top of the valence band (TVB) and the internally confined state at the bottom of the conduction band (BCB) to define the gap instead of HOMO and LUMO because there may be many occupied dangling bond states between the TVB and the BCB.

In the Harris functional, electrons are not shared between atoms; therefore, the molecular orbitals associated with the dangling bonds have energies near the energy gap. The transfer of electronic charge from one atom to another in DOGS causes the energies of the dangling bonds to shift further into the gap region. Thus, both Harris and DOGS obscure our finding at the TVB and BCB because the dangling bonds reside around the band edges.[12]

The purpose of this work is to understand how surface relaxation affects the band gap; to do so, we must first estimate the TVB and BCB states for each nanocrystal. To find the TVB and BCB states we take out the atoms that have dangling bonds by species and then perform a single-point calculation by using the Harris functional (i.e., we use the lattice structure and self-consistent potential previously found for the full structure, remove the surface atoms of a particular species, and then recalculate the states with those surface atoms removed, without iterating to self-consistency). Removing all of the sulfur atoms that have dangling bonds (leaving only cadmium dangling bonds) will yield an estimate of the TVB energy. Similarly, by removing all of the surface cadmium atoms, we obtain an estimate for the BCB energy. Removing the atoms by species is similar to adjusting the potentials associated with surface atoms, as was done by Díaz *et al.*[24] This produces crystal structures that are slightly smaller with fewer atoms and an estimated energy gap that should be slightly larger than the TVB-BCB difference of the nanocrystal. We use this procedure on both the zinc-blende (ZB) and relaxed configurations of the nanocrystals.

Surface relaxation plays a big role in the number and type of dangling bonds. To achieve the proper surface relaxation, we will first perform a quenching procedure where we use the Harris functional for a number of optimization time steps followed by an optimization run using DOGS. The reason we use this two step process is that cleaving the perfect crystal produces an immediate metallization of the surface due to dangling bonds. The metallization of the surface becomes more pronounced as the charge transfer involved in the bonding process increases. A proper charge configuration can only be obtained via a self-consistent field (SCF) calculation; however, a SCF calculation on the ZB structure of our nanocrystals fails to converge. Therefore, we use a non-SCF optimization procedure, like the Harris functional within FIREBALL, to allow for surface relaxation and to remove this surface metallization. After the initial relaxation, we allow further relaxation with SCF turned on.

In modeling the nanocrystals, we used a $4d^{10}5s^2$ basis for Cd and a $3s^23p^4$ basis for S with Hamann-type pseudopotentials[30] with the Horsfield exchange-correlation approximation.[29] Cutoff radii used for the sulfur atoms are $r_c^s=0.42$ nm and $r_c^p=0.47$ nm, and those for the cadmium atoms are $r_c^s=0.51$ nm, $r_c^p=0.50$ nm, and $r_c^d=0.45$ nm. To find the band gap of the unrelaxed ZB structures, we removed the surface atoms by species and ran a single-point calculation

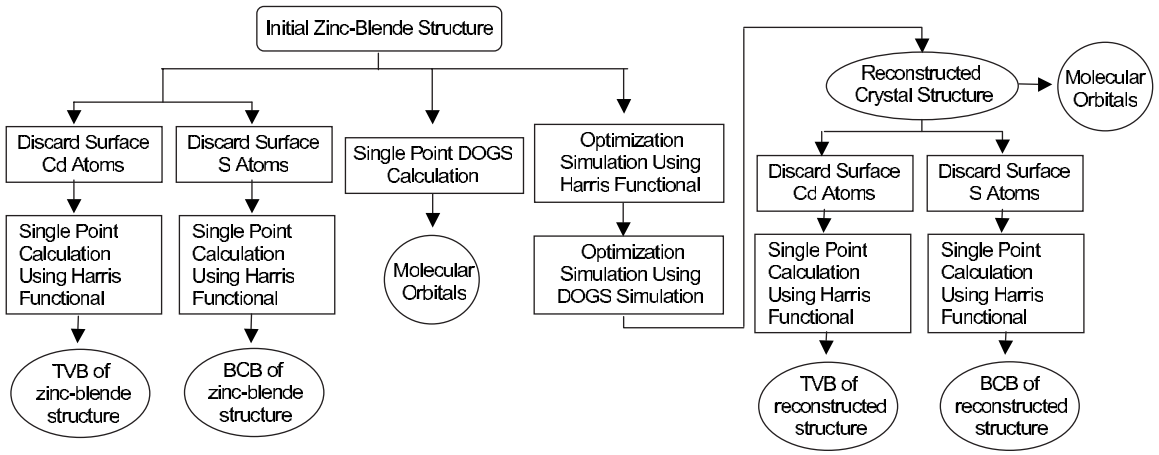

FIG. 1. This flowchart shows the steps used to obtain our results; the rectangles represent specific calculations or simulations performed and the ovals represent results.

by using the Harris functional; this procedure is similar to that proposed in Ref. 19. We relax the nanocrystal with a 600 time-step (2.00 fs for each step) molecular dynamics simulation by using the Harris functional for each nanocrystal. Starting from that relaxed configuration, we perform an additional 600 time-step SCF simulation, each time step of which was allowed a maximum number of 20 SCF steps. In the cases of both the relaxation using the Harris functional and the relaxation using DOGS, the root-mean-squared forces were less than 1.0 eV/nm. To find the band gap of the fully relaxed structures, we remove the surface atoms by species, as described above, and run the single-point calculation by using the Harris functional. A flow chart showing the procedures used in obtaining our results can be found in Fig. 1, and the purpose of each step will be given below.

The spatial localization of a molecular orbital can be defined by identifying the charge localized on bulk and surface atoms, where the surface atoms in an unrelaxed ZB structure are those atoms with less than four nearest neighbors. The bulk (surface) probability for a state is the probability that the state is on the interior (surface) atoms. However, in a relaxed structure, the assignment of nearest neighbors is more arbitrary, so the assignment of surface and bulk atoms may not be clear cut and the separation of bulk and surface contributions may become more problematic. We will define below the number of accessible atoms W to quantify the degree of spatial localization.[31] The Mulliken charge, $p_i(\nu)$, is the probability that an electron in state ν can be found at atom i, and we note that the sum over all atoms of $p_i(\nu)$ would equal 1 for each state, $\Sigma_i p_i(\nu)=1$. By using $p_i(\nu)$, we can calculate the entropylike quantity:

$$S(\nu) = -\sum_i p_i(\nu) \ln p_i(\nu), \tag{1}$$

where the sum is defined over all atoms, in the system. The number of accessible atoms, $W(\nu)$, is thus defined as

$$W(\nu) = e^{S(\nu)}. \tag{2}$$

This definition is independent of any definition of the nearest neighbor atoms. If the charge is spread uniformly over M atoms, then $W=M$. If the charge is localized to a single atom, then $W=1$. We will use W to show that the dangling bond states are associated with only a few atoms.

III. BULK BAND STRUCTURE

As the first step in establishing the validity of our results, we present a band structure for bulk CdS computed by using FIREBALL. We first find the lattice constant a that minimizes the total energy per atom by using the Harris functional to compute the total energy per atom for a spread of values around the experimental value of a. By searching in the range $a=[0.57,0.59]$ nm, this procedure gave a value of $a=0.584$ nm, which is comparable to the experimental value of $a=0582$ nm.[32] From the computed lattice constant, we calculate the band structure of the ZB structure; see Fig. 2(a). We find a direct band-gap energy of 1.96 eV at the Γ point, which is similar to the value of 2.01 eV computed by Zunger and Freeman[33] by using a linear-combination-of-atomic-orbitals technique. The experimental value of the band gap is 2.50 eV from reflectivity[34] or 2.4 eV from ellipsometry.[35] This discrepancy is expected for a DFT calculation. Using a plane wave basis set, DFT in the local density approximation would give band-gap values of about half of the experimental value. However, using localized orbitals, which have slightly excited energy eigenvalues in an incomplete basis, offsets the errors inherent to DFT and increases the band gap. From the band structure, we calculated the hole and electron effective masses, giving a heavy hole effective mass of $0.76m_e$ and an electron effective mass of $0.14m_e$; the heavy hole falls within the range of experimental values $(0.53m_e-0.8m_e)$ while the electron is approximately 26% off of experiment $(0.18m_e-0.2m_e)$.[36]

Díaz *et al.*[24] calculated the band structure of CdS by using a semiempirical tight-binding calculation. We compare the band structure that we have computed by using the FIREBALL method, Fig. 2(b), to their band structure computed by using the sp^3d^5 model, Fig. 2(c).[37] In comparing the two band structures, we find that both have the same general features. The band structure of Díaz *et al.* is fitted to experimental

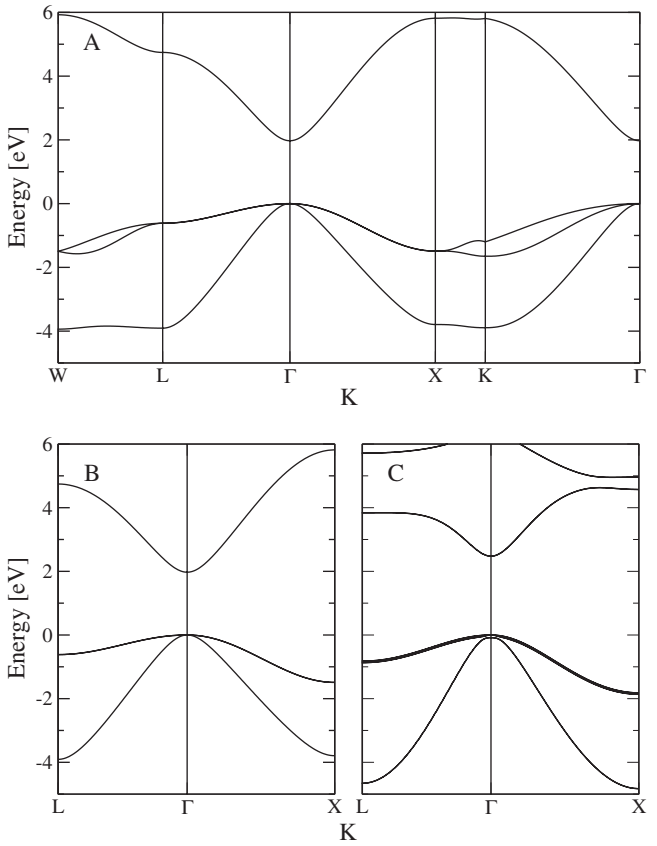

FIG. 2. [(a) and (b)] Band structure of the ZB structure of CdS as produced by FIREBALL. (c) Band structure produced by Díaz *et al.* by using a semiempirical method. The light hole line will resolve into two lines upon resizing the figure.

values so that it yields the correct band gap. It also takes into account electron spin, which produces a split off band [this can be observed by rescaling Fig. 2(c)]. The FIREBALL method is a ground state method, so the shapes of the heavy and light hole curves around the Γ point tend to be more accurate.

From the results we have just presented, we believe that our model of CdS has validity and that we can continue on to look at nanocrystal structures.

IV. SURFACE RELAXATION

For use in this work, six spherical CdS nanocrystals were considered, all initially in the ZB structure. These included a bond centered nanocrystal with radius $2a$, $Cd_{132}S_{132}$ (CdS264); and five atom centered nanocrystals: with radii of 1.168 nm, $Cd_{140}S_{140}$ (CdS280); 1.168 nm, $Cd_{140}S_{141}$ (CdS281); 1.168 nm, $Cd_{152}S_{141}$ (CdS293); 1.2556 nm, $Cd_{152}S_{177}$ (CdS329); and 1.267 28 nm, $Cd_{180}S_{177}$ (CdS357). We will hereafter reference each nanocrystal by the designation given in parentheses. We chose to do crystallites CdS264 and CdS281 because they have the same radius but have different numbers of atoms. Nanocrystal CdS280 was created by taking one of the S atoms off of the surface of CdS281 in order to have a second stoichiometric system. In the ZB structure, a bulk atom will have four nearest neighbors; we will therefore define any atom in the unrelaxed structure with less than four nearest neighbors as a "surface atom." That designation is assumed to apply even after relaxation.

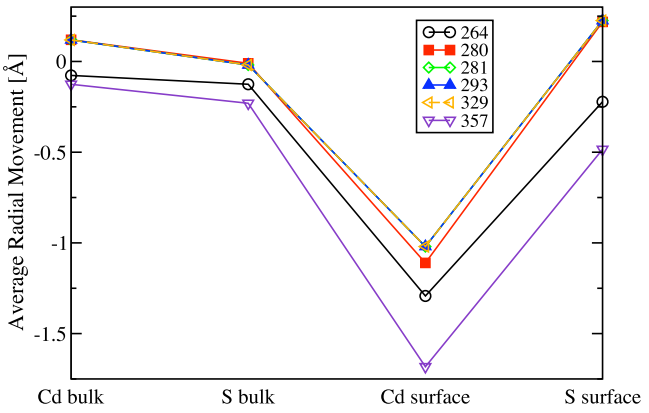

FIG. 3. (Color online) Average radial movement of atoms after the surface reconstruction.

Figure 3 shows the average radial displacement of the atoms in each of the nanocrystals after we perform the relaxation process. The interior atoms tend to only slightly move. However, on the surface, the Cd atoms move inward on the order of 0.1 nm and the S atoms tend to move outward as they are displaced by the inward moving cadmium. In the cases of nanocrystal CdS264 and nanocrystal CdS357, we find that the surface S atoms slightly move inward; this is apparently because the Cd atoms move in toward the center of the nanocrystal by such a large amount. In all the cases, the change in volume of the nanocrystal is minimal. Similar results have been found by others for CdS as well as other type II–VI systems.[9,12,13,20,38,39] The relative displacements of the atoms are consistent with basic principles of chemical bonding. Because of the large electron affinity of the S atoms, they form covalent bonds with the electrons in the filled valence shells of the Cd atoms, driving the Cd atoms on the surface to move deeper into the nanocrystal in an attempt to reclaim a filled orbital state, creating a S rich surface.

In Fig. 4, we present the initial positions of the atoms in a bulklike ZB lattice and their final positions after relaxation. The atoms near the center of the nanocrystals only slightly move leaving them in a roughly ZB structure after the relaxation process. We also find that in the interior of the nanocrystals, the relaxation process may bring a Cd atom (one that had been on the surface in the ZB structure) into a position where its distance from an S atom, other than its ZB nearest neighbors, is about 10% longer than the nearest neighbor bonds in a ZB structure, thus becoming a fifth neighbor for that S atom. Finally, we do not observe the formation of S-S or Cd-Cd bonds.

V. MOLECULAR ORBITAL STATES

In Ref. 19, Bryant and Jaskolski used an empirical tight-binding method to study unrelaxed CdS ZB nanocrystals. In their work, they considered four models for surface passivation: no passivation, only Cd dangling bonds passivated,

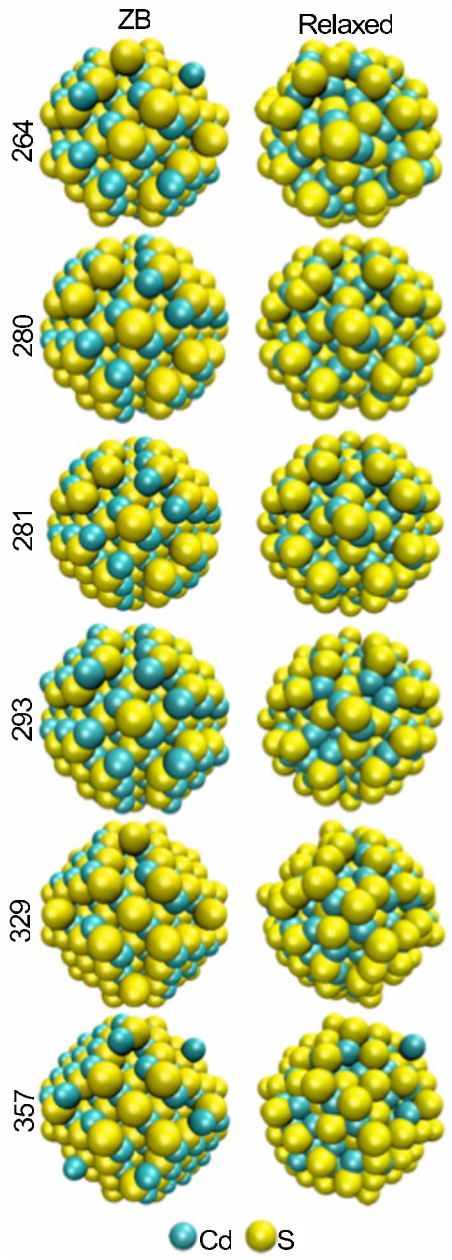

FIG. 4. (Color online) Surface realignment. The left (right) hand column shows each nanocrystal in its ZB (relaxed) configuration. Each row has a different size of the nanocrystal. The top row is the CdS264 structure with more atoms in each structure going down each column.

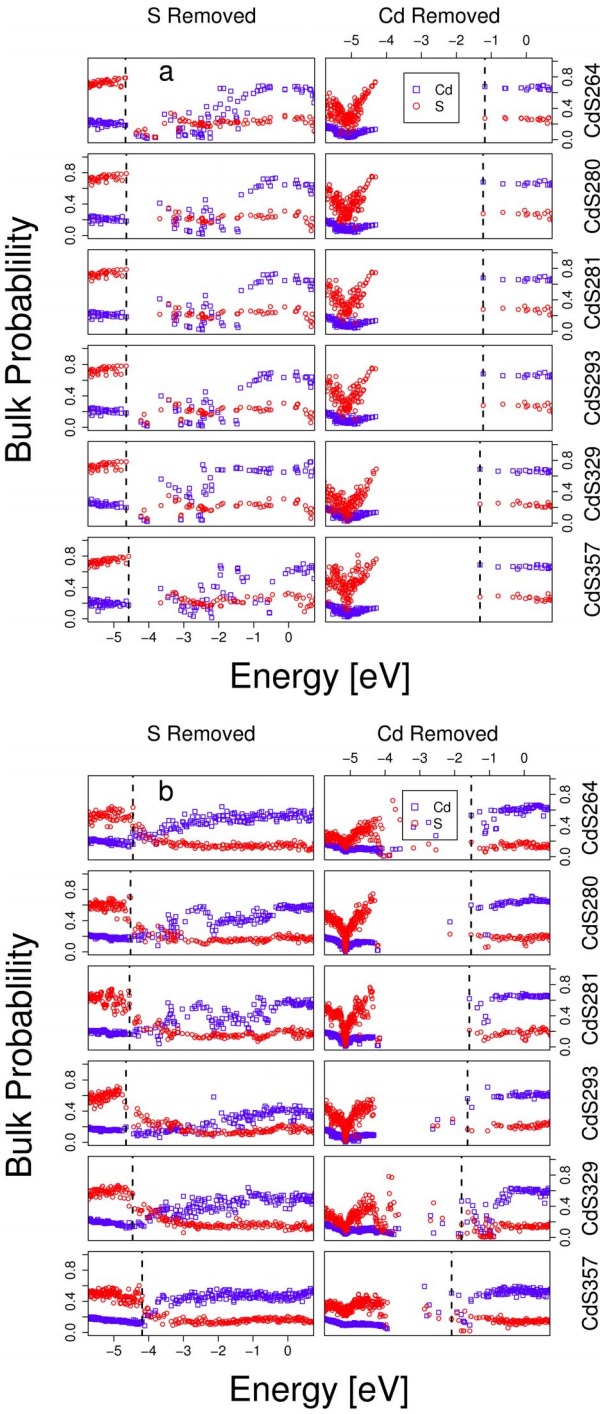

FIG. 5. (Color online) Determination of the gap energy for each crystal in both (a) the unrelaxed ZB structure and (b) the relaxed structure. The probability to be on bulk Cd atoms [dark gray (blue) squares] and bulk S atoms [light gray (red) circles] are shown for each single-particle state near the gap. The TVB and BCB are indicated by dashed lines. The left frames are the result of a single-point calculation by using the Harris functional when surface S atoms are removed and there are only Cd dangling bonds (used to define the TVB energy) and the right frames are the result when Cd surface atoms are removed, leaving the S dangling bonds (used to define the BCB energy). Notice in (a) that there is a slight shifting in the TVB and BCB energies such as the increase in energy gap as the number of atoms is reduced.

only S dangling bonds passivated, and both Cd and S dangling bonds passivated. Passivation is modeled by shifting the energy of the dangling bonds, V_{db}, so that gap states are shifted well above (or below) the other bands, leaving only internally confined states near the band gap. By effectively passivating the dangling bonds in this manner, they were able to calculate a band gap without the added complexity of adding a capping layer. By plotting the bulk probability for different levels of passivation, they show how the band gap was influenced by the dangling bonds, as well as discuss where in the nanocrystal any gap states reside. We benchmark our results to those of Bryant and Jaskolski by remov-

TABLE I. Number of Cd and S atoms in the resultant crystal when surface atoms are taken off the ZB structures.

	Original		S removed		Cd removed	
System	No. of Cd	No. of S	No. of Cd	No. of S	No. of Cd	No. of S
CdS264	132	132	132	71	71	132
CdS280	140	140	140	83	80	140
CdS281	140	141	140	83	80	141
CdS293	152	141	152	83	80	141
CdS329	152	177	152	83	104	177
CdS357	180	177	180	111	104	177

ing all surface atoms of the same species. Effectively, this removes all dangling bonds related to that species. From our results, we will identify the TVB and the BCB, allowing us to determine how the gap states derived from dangling bonds affect the band gap.

Before looking at the relaxed systems, we will consider how removing the surface atoms by species affects the nanocrystals while in their zinc-blende configuration. Doing so will allow us to test this technique on systems similar to those in Ref. 19 and later compare the results to those of the relaxed structures. Our procedure slightly differs from that used by Bryant and Jaskolski. In their procedure, the surface atoms and the backbonds remain after the dangling bonds are removed. In our approach, the surface becomes either Cd or S rich, with only Cd or S dangling bonds. The removal of the S derived states allows us to identify TVB, while removal of the Cd derived states allows us to identify the BCB.

In Fig. 5(a), we show the probabilities to be on bulk Cd and S atoms for each state near the gap. In the left hand panels, we plot the bulk probability when the S atoms have been removed and in the right hand panels, we plot the hulk probability when all of the surface Cd atoms have been removed. We have results similar to those of Ref. 19. From these results, we identify the TVB and the BCB. Table I presents the number of atoms remaining after the atoms were removed by species. We choose the TVB to be the highest valence state with a large probability to be on bulk S atoms, just before the bulk S probability drops as the molecular orbitals become surface states. Similarly, the BCB state should be the lowest conduction-band state with a high probability to be on bulk Cd atoms. The dashed lines in the left and right hand panels pass through the TVB and BCB, respectively. In the left hand panels of Fig. 5(a), states below the TVB look remarkably like the valence states of Ref. 19. In the right hand panels, we find that the states to the right of the dashed line look like the conduction states of Ref. 19. The TVB and BCB energies and band gaps for the ZB structures of the nanocrystal systems studied are given in Table II.

In the ZB structure, we find that the band gap generally decreases as the size of the particle increases. We see a minor exception to this when going from CdS280 to CdS281 where the band gap increases by 0.04 meV, or about 0.001%, which lies within the tolerances of the present computational method and any variations expected for discrete atomistic effects. A more notable exception occurs when comparing the band gaps of CdS281 and CdS293. In this case, there is a jump in the number of Cd atoms, and one would expect this to make the crystalline more metallic and would expect this to decrease the band gap. This effect is the only instance we have seen in our analysis where lack of stoichiometry has a noticeable effect.

Assigning the TVB and BCB states for the nanocrystals in the ZB structures is straight forward once the bulk probability is determined. The same is not true for the relaxed structures. For the relaxed structures, there are more, rapid variations in the bulk probability because some states that were degenerate in the ZB structures can become nondegenerate in the relaxed structures. In making our choice of where the TVB and BCB are in the relaxed structures, we have used the following reasonable guidelines: (1) The bulk probability of the Cd atoms and of the S atoms each had to follow the trend set by the unrelaxed ZB nanocrystals; for example, when the

TABLE II. Energy of the TVB and BCB and the band gap for nanocrystals in the ZB configuration.

System	TVB (eV)	BCB (eV)	Gap (eV)
CdS264	−4.66644	−1.18442	3.48202
CdS280	−4.64307	−1.23413	3.40894
CdS281	−4.64307	−1.23409	3.40898
CdS293	−4.64744	−1.23409	3.41335
CdS329	−4.64744	−1.32342	3.32402
CdS357	−4.57584	−1.32342	3.25242

TABLE III. Energy of the TVB and BCB and the band gap for nanocrystals in the relaxed configuration.

System	TVB (eV)	BCB (eV)	Gap (eV)
CdS264	−4.45219	−1.52261	2.92958
CdS280	−4.52048	−1.52794	2.99254
CdS281	−4.55150	−1.57639	2.97511
CdS293	−4.65063	−1.62789	3.02274
CdS329	−4.46160	−1.80015	2.66145
CdS357	−4.18726	−2.08743	2.09983

TABLE IV. Number of Cd and S atoms in the resultant crystal when surface atoms are taken off the relaxed structures.

	Original		S removed		Cd removed	
System	No. of Cd	No. of S	No. of Cd	No. of S	No. of Cd	No. of S
CdS264	132	132	132	66	89	132
CdS280	140	140	140	81	90	140
CdS281	140	141	140	77	76	141
CdS293	152	141	152	77	76	141
CdS329	152	177	152	78	104	177
CdS357	180	177	180	118	142	177

surface Cd atoms were removed, the value for Cd and S had to be around 0.6 and 0.3, respectively. (2) The energy of the TVB and BCB could not be radically different from the trends for the unrelaxed structures that are easier to judge. With these criteria in mind, we determined the TVB and BCB. The results are given in Table III and in Fig. 5(b) with the number of atoms used in determining the TVB and BCB given in Table IV.

Explanation of the determination of the TVB and BCB in the relaxed structure cases may convince the reader of the validity of the energy values that we put forth. Since the cases where the Cd atoms are removed are simpler to justify, we will concern ourselves with them first. By observing CdS264 and CdS281 in Fig. 5(b) we see that states basically resemble the bulk probability of the bulklike configurations, thus, the lowest energy state above the gap should be the BCB. In CdS280, we would have a similar case if not for the one state at −2.134 81 eV, this one state is not the BCB because it does not fit condition (1) or (2) described in the previous paragraph. Similarly, in CdS293, the three states between −3 and −2 eV do not fit either condition. The value determined in CdS329 is harder to come by. Here, we have the bulk probability of the Cd and S atoms separated well as we found in the bulk like case at higher energies and then as we go to slightly lower energies, they both become much lower before rising again. The dip in values is due to surface states crowding into the conduction band as bonds are passivated. Again, there are three states that are in the (−3,−2) eV range, which we will ignore. There also happens to be two states with energies just lower than the state we have determined to be the BCB for CdS329, neither of these are candidates because they are both surface states and thus fail condition (1). CdS357 is similar to CdS329 in that there are a few surface states that have moved into the conduction band, there are also three states in the (−3,−2) eV range that fail for reasons mentioned above, the difference is that there is also a fourth state near −3 eV, which has the correct form for the bulk probability but it fails condition (2).

Determining the TVB is harder due to noise from the unbounded Cd atoms throughout the whole band gap. For CdS264, CdS280, CdS281, CdS329, and CdS357, the determination of which state is the TVB is fairly easy because the last state that follows the valence band pattern set by the ZB systems also has a high S bulk probability, immediately after which the states have Cd and S bulk probabilities that are close together, signifying a fundamental difference in the type of state. CdS293 is the only one which is questionable. For CdS293, we find the bulk probability of the three states with the highest energies before a small gap in states that move closer together, mimicking the trend that we find in the slightly higher energy states after the gap. Ultimately, we decided that the last state is the TVB so as to most closely follow our second guideline.

While the fluctuation that we observe in the gap energy with change in crystal size is not fully understood, the literature has a number of examples of other groups seeing the same type of effect. Roy and Springborg showed fluctuations of the LUMO of up to about 0.5 eV, with fluctuations of 0.1–0.2 eV for the HOMO in indium phosphide clusters.[38] Their energy gap tops (bottoms) out at about 1 (0.3) eV for ZB and about 1.3 (0.6) eV for wurtzite. Similarly, for Cd_mSe_n, results from Sarkar and Springborg,[13] from Troparevsky *et al.*,[40] and from Yu *et al.*[17] show that some nanocrystals of up to a few hundred atoms have gaps that are near the band-gap energy of bulk CdSe. Pal *et al.*[39] showed that for Zn_mS_n, the LUMO may fluctuate by almost 1 eV as the number of atoms increase. Lippens and Lannoo[34] in Fig. 1 showed a nonmonotonic decrease in the band gap with increasing number of atoms. The band gap produced by semiempirical tight-binding calculations is generally close to the empirical band gap of a system because they change their parameters to fit it. This might explain why they get much smaller fluctuations in the energy of the LUMO state, with the energy gaps they find for CdS and ZnS staying near the experimental values obtained for the respective nanocrystals.

TABLE V. Number of states in the energy gap for each system in the ZB structure and in the relaxed structure, along with the band-gap energies of the structures.

Atoms	No. in ZB	ZB gap (eV)	No. in relax	Relax gap (eV)
CdS264	123	3.48202	58	2.92958
CdS280	123	3.40894	77	2.99254
CdS281	122	3.40898	73	2.97511
CdS293	121	3.31335	54	3.02274
CdS329	74	3.32402	65	2.66145
CdS357	171	3.25242	44	2.18476

Joswig *et al.*[20] showed that the gap can fluctuate by as much as 2 eV for CdS. Furthermore, as with our results, they end up with gap values that near the bulk limit.

Joswig *et al.* stated that they find that the BCB is localized between one and three surface atoms, and thus, the LUMO very sensitively depends on variations in the cluster surface. They further argued that the experimental results of Lifshitz *et al.*[41,42] support their claim. The fact that we find in some cases, the energy gap between the TVB and BCB to be near our computed bulk limit for the band gap is related to the inherent difficulties of trying to determine a value that is obscured by a strong dependence on the coordination of the atoms.

Turning now to a comparison of the bulklike ZB structures and the relaxed structures, we find that in each case there are fewer states within the energy gap when the crystal is in the relaxed configuration than when the same nanocrystal is in the unrelaxed ZB configuration; Table V gives the number of states found in the gap region for each crystallite structure before and after reconstruction.

In Fig. 6(a), we present the bulk probability of the ZB structure as found by the single-point SCF calculation, and of the relaxed structure, after the 600 time, step DOGS calculation. In Fig. 6(b), we give the number of atoms on which each state might be found as defined by the number of accessible atoms [Eq. (2)]. For the ZB structure, most of the gap states were near the valence band edge. These gap states are seen to be near the surface and most were spread over no more than 50 atoms. The gap states increasingly became bulklike and increasingly delocalized toward the band edges. Once the crystallites are relaxed we find that there are many fewer states in the gap and most are near the conduction-band edge. After relaxation, the states near the valence band edge become even more localized and more fully reside on the surface. The gap states near the conduction band edge are delocalized and nearly equally distributed over the surface and bulk atoms. The change in the number of states near the band edges along with the changes in the bulk probability and the characteristic number of accessible atoms for each state restores the semiconductor properties of the surface that was destroyed when the ZB was cleaved, forming the spherical nanocrystal.

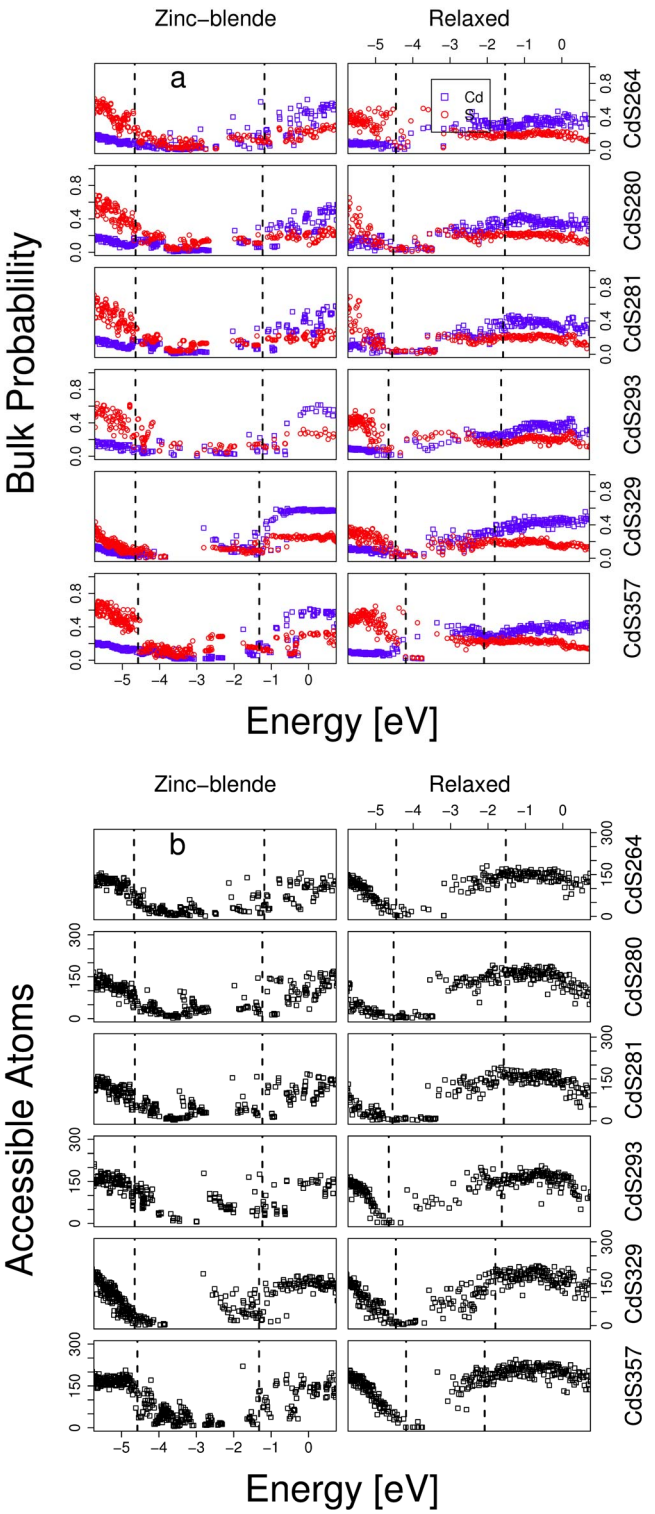

FIG. 6. (Color online) Graphs showing (a) the bulk probability and (b) the number of accessible atoms both before and after optimization. The dashed lines specify the TVB and BCB energies of the respective systems.

VI. SUMMARY

We have found that the reconstruction process has broken the point symmetries of the crystal in its ZB structure, partially passivated the surface of the nanocrystal (decreasing the number of gap states), and that the gap states are mostly surface states.

In a bulk crystal, we would find that the HOMO, and the states just below the HOMO, would be localized, while the LUMO, and those states just above, would be highly delocalized. We have found that upon cleaving the bulk zinc-blende structure into a nanocrystal, with the atoms still in a zinc-blende configuration, the valence states are less localized, while the conduction states are more localized. After relaxation, the valence states are again localized while the conduction states are more delocalized. Thus, the relaxation process has restored the semiconductor nature of the nanocrystal.

ACKNOWLEDGMENTS

This research is funded in part by the National Institute of Standards and Technology Grant No. 70NANB7H6008. The molecular dynamics simulations used in the relaxation of the nanocrystals in this work were performed at the Ira and Marylou Fulton Supercomputing Laboratory at Brigham Young University. This work was supported in part by a grant from the West Virginia Graduate Student Fellowships in Science, Technology, Engineering and Math (STEM) program.

*Also at the Department of Physics and Astronomy, Brigham Young University, Provo, UT 84602, USA; chad.junkermeier@mail.wvu.edu

[1] M. G. Bawendi, M. L. Steigerwald, and L. E. Brus, Annu. Rev. Phys. Chem. **41**, 477 (1990).
[2] J. Ouellette, Ind. Phys. **9**, 14 (2003).
[3] S. Pokrant and K. B. Whaley, Eur. Phys. J. D **6**, 255 (1999).
[4] N. A. Hill and K. B. Whaley, J. Chem. Phys. **99**, 3707 (1993).
[5] N. A. Hill and K. B. Whaley, J. Chem. Phys. **100**, 2831 (1994).
[6] S. Yokojima, T. Meier, and S. Mukamel, J. Chem. Phys. **106**, 3837 (1997).
[7] H. H. von Grünberg, Phys. Rev. B **55**, 2293 (1997).
[8] K. Leung, S. Pokrant, and K. B. Whaley, Phys. Rev. B **57**, 12291 (1998).
[9] K. Leung and K. B. Whaley, J. Chem. Phys. **110**, 11012 (1999).
[10] K. Eichkorn and R. Ahlrichs, Chem. Phys. Lett. **288**, 235 (1998).
[11] K. E. Andersen, C. Y. Fong, and W. E. Pickett, J. Non-Cryst. Solids **299-302**, 1105 (2002).
[12] P. Deglmann, R. Ahlrichs, and K. Tsereteli, J. Chem. Phys. **116**, 1585 (2002).
[13] P. Sarkar and M. Springborg, Phys. Rev. B **68**, 235409 (2003).
[14] B. Goswami, S. Pal, P. Sarkar, G. Seifert, and M. Springborg, Phys. Rev. B **73**, 205312 (2006).
[15] L. W. Wang and A. Zunger, Phys. Rev. B **53**, 9579 (1996).
[16] A. Puzder, A. J. Williamson, F. Gygi, and G. Galli, Phys. Rev. Lett. **92**, 217401 (2004).
[17] M. Yu, G. W. Fernando, R. Li, F. Papadimitrakopoulos, N. Shi, and R. Ramprasad, Appl. Phys. Lett. **88**, 231910 (2006).
[18] M. Troparevsky and J. R. Chelikowsky, J. Chem. Phys. **114**, 943 (2001).
[19] G. W. Bryant and W. Jaskolski, J. Phys. Chem. B **109**, 19650 (2005).
[20] J. Joswig, M. Sringborg, and G. Seifert, J. Phys. Chem. **104**, 2617 (2000).
[21] J. Joswig, G. Seifert, T. A. Niehaus, and M. Sringborg, J. Phys. Chem. B **107**, 2897 (2003).
[22] G. W. Bryant and W. Jaskolski, Phys. Rev. B **67**, 205320 (2003).
[23] R. B. Little, M. A. El-Sayed, G. W. Bryant, and S. E. Burke, J. Chem. Phys. **114**, 1813 (2001).
[24] J. G. Díaz, M. Zielinski, W. Jaskolski, and G. W. Bryant, Phys. Rev. B **74**, 205309 (2006).
[25] J. P. Lewis, K. R. Glaesemann, G. A. Voth, J. Fritsch, A. A. Demkov, J. Ortega, and O. F. Sankey, Phys. Rev. B **64**, 195103 (2001).
[26] P. Jelínek, H. Wang, J. P. Lewis, O. F. Sankey, and J. Ortega, Phys. Rev. B **71**, 235101 (2005).
[27] J. Harris, Phys. Rev. B **31**, 1770 (1985).
[28] A. A. Demkov, J. Ortega, O. F. Sankey, and M. P. Grumbach, Phys. Rev. B **52**, 1618 (1995).
[29] A. P. Horsfield, Phys. Rev. B **56**, 6594 (1997).
[30] D. R. Hamann, Phys. Rev. B **40**, 2980 (1989).
[31] J. P. Lewis, J. Pikus, T. E. Cheatham, E. B. Starikov, H. Wang, J. Tomfohr, and O. F. Sankey, Phys. Status Solidi B **233**, 90 (2002).
[32] *Numerical Data and Functional Relationships in Science and Technology*, edited by K. H. Hellwege and O. Madelung, Landolt-Börnstein, New Series, Group III, Vol. 17, Pt. b (Springer, Berlin, 1982).
[33] A. Zunger and A. J. Freeman, Phys. Rev. B **17**, 4850 (1978).
[34] M. Cardona, M. Weinstein, and G. A. Wolff, *Ultraviolet Reflection Spectrum of Cubic CdS*, MRS Symposia Proceedings No. 140 (Materials Research Society, Pittsburgh, 1965), pp. A633–A637.
[35] B. Pradhan, A. Sharma, and A. K. Ray, J. Nanosci. Nanotechnol. **5**, 1130 (2005).
[36] P. E. Lippens and M. Lannoo, Phys. Rev. B **39**, 10935 (1989).
[37] S. Sapra, N. Shanthi, and D. D. Sarma, Phys. Rev. B **66**, 205202 (2002).
[38] S. Roy and M. Springborg, J. Phys. Chem. **107**, 2771 (2003).
[39] S. Pal, B. Goswami, and P. Sarkar, J. Chem. Phys. **123**, 044311 (2005).
[40] M. C. Troparevsky, L. Kronik, and J. R. Chelikowsky, Phys. Rev. B **65**, 033311 (2001).
[41] E. Lifshitz, I. Dag, I. Litvin, S. Gorer, R. Reisfeld, M. Zelner, and H. Minti, Chem. Phys. Lett. **288**, 188 (1998).
[42] E. Lifshitz, I. Dag, I. D. Litvin, and G. Hodes, J. Phys. Chem. B **102**, 9245 (1998).